UDC 621.39

Improvement of Eddy Current Control System and Response Signal Analysis Model to Increase the Informativeness of Metal Identification

Abramovych A. O., Bazhenov V. G.

National Technical University of Ukraine "Igor Sikorsky Kyiv Politechnic Institute", Kyiv, Ukraine

E-mail: osslo@ukr.net

The paper examines the results of metal object identification using an eddy current dynamic control system based on the amplitude-phase method of processing the response from the object under study. The article proposes an improved signal-response model of the eddy current dynamic control system. The considered aspects of the implementation of the dynamic control process allowed us to improve the previously proposed analytical model of signal-response description, thanks to which it now takes into account the electrical and magnetic characteristics of metals analytically, and not by approximating the shape of the response signal as in the previous model.

The work emphasizes that an important variable of the model is the speed of passing a metal object over the antenna plane. The speed affects the shape of the signal-response and the information coefficients calculated later. A study was conducted to determine the optimal speed of passing a metal object over the antenna surface, which corresponds to the range of linear speeds of 4...6 m/s.

Metal identification using several different rotation frequencies is better and more accurate, as it allows for a more informative characterization of an unknown new sample and to determine which ones it is most similar to.

The investigation for determine the optimal rotation frequency of metal objects above the antenna plane allowed to increase the informativeness of the system, as evidenced by the increase in the correlation difference when distinguishing metals, for example, copper and other metals, from 10-15% to 20-25%, for example, tantalum from 8-12% to 15-20%, and cobalt from 10-12% to 20%.

Keywords: electromagnetic properties of metals; eddy current system; STM32H745 microcontroller; identification of metals; mathematical modeling; amplitude-phase method of signal registration; STM32; metal detector

DOI: 10.20535/RADAP.2025.101.51-59

Introduction

The problem of remote identification of metal objects is relevant for a number of practical applications [1]. Various methods are used to solve it, in particular, X-ray, optical emission, eddy current [1]. The use of the eddy current dynamic control system (ECS) proposed in [2] is quite effective [3].

A number of works [3–5] are devoted to the processes of signal formation in eddy current devices, but they do not fully explain the peculiarities of the occurrence of the response signal and its shape.

This publication presents the results of measurements based on the proposed improved ECS and the analytical model of signal-response description from metal objects, which were carried out using the ECS improved by the authors [2]. ECS is built on the basis of circuit solutions of input stages used in metal detectors (signal generator, output amplifier,

low-noise input amplifier and phase detector) [3], and a microcontroller. Metal identification is carried out using software built on the basis of the signal processing technique proposed in [2,3].

- 1 Mathematical model of response signal formation in the eddy current method
- 1.1 Description of the improved eddy current system of the dynamic control method

There are a number of mathematical models that explain the operation of the eddy current method of detecting metal objects. In particular, these are the Bruschini model [4], the model of A. Yu. Grinyev [6] and the model of the theory of non-destructive

testing [7]. A specially improved eddy current testing system (ECS) was used to carry out the research.

The structural diagram of the modernized ECS is shown in Fig. 1 [3, 8]. The ECS consists of an

antenna system (transmitting and receiving coils), a low-frequency signal generator, signal amplification and processing units, a clock generator, a microcontroller, and an indicator device.

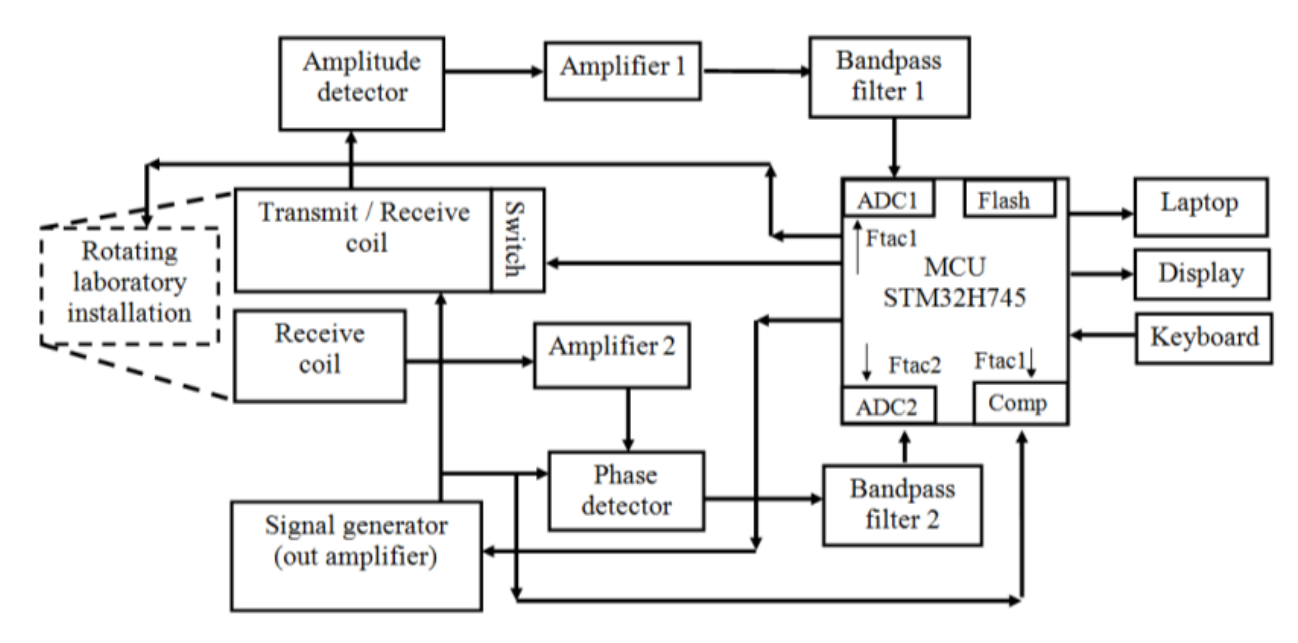


Fig. 1. Structural diagram of the modernized system

The low-frequency signal generator [9] generates signals in the kilohertz range (6.6 kHz), which, using a transmitting coil, emit an electromagnetic field into the studied medium. As a result of electromagnetic induction, Foucault currents (surface currents) arise on the surface of the studied metal object and them generating secondary electromotive force (EMF), which are received by the receiving coil [10], cause a response signal in it and are fed to the amplification and primary processing unit.

Synchronization between nodes is provided by a clock pulse generator (output amplifier) and a microcontroller STM32H745.

The system can operate in two modes: Dynamic and Static and emit two types of signals, respectively: tone and pulse. The microcontroller switches the operating modes of the transmitting coil, so that it can emit either tone or pulse signals.

The emission of a pulse signal is required if the metal sample is too large and cannot be examined dynamically—the measurement is carried out through an amplitude detector. The measurement of phase characteristics is carried out by multiplying digitized samples from the ADC1 and the comparator, the samples are taken with the frequency Ftac1. According to the signals of the microcontroller, the initial phase of the probing signal can be changed and, through the feedback loop through the comparator, the changed signal can be fed to the microcontroller and multiplied with the signals from the ADC1 in the pulse mode of

operation (this is how the phase detector of the pulse signal is implemented, which operates either in binary mode, i.e. by detecting zero crossings) – this is how the phase characteristics for large metal samples are measured.

In the dynamic mode of operation of the ECS, the signal from the output amplifier is fed to the amplitude-phase detector and the transmitting coil with tone signals and digitizes them through ADC2 with a frequency of Ftac2.

After multiplication in the phase detector, the analog signal is digitized and fed to the microcontroller unit. The dynamic range of the microcontroller's ADC is about 84 dB [11]. In the microcontroller, the signals received from the samples under study are compared with a library of reference signals [2, 3], which are stored in the microcontroller's memory. The comparison result is fed to the indicator device. The modernized ECS is built on a dual-core STM32H745 microcontroller. The first core controls the operation of the eddy current unit, the second core converts the measured data into the format required for further transmission to the indicator device (HP 4540s laptop). At this stage of development, all processing is carried out on the laptop, the keyboard and display are used for visual control of the ECS operating modes, and the possibility of writing digitized samples to flash memory is also provided.

In the future, the program code for the microcontroller will be added so that all processing takes

place only on the basis of the built-in STM32H745 cores (M7 and M4) and there is no need to use a laptop – then the system will have two options for use:

- stationary system for dynamic control of the composition of metals or alloys;
- portable metal detector with the ability to distinguish metals by type (unlike modern metal detectors that distinguish between magnetic / non-magnetic) [2,3].

Information is transmitted to a personal computer in 16-bit packets [12, 13]. A USB port is used for connection. The PC is equipped with the MATLAB application package, in which, using the response signal amplitude normalization program and computer programs for graphic-digital imaging and spectral methods, classification features are numerically determined.

Dynamic scanning of a metal object is carried out by a rotating laboratory setup, which allows stabilizing the relative movement of the antenna system and the metal under study, and allows changing the relative speed of movement of objects in a plane parallel to them.

Therefore, in the designed experimental system, the reflected signal is its relative characteristic, which becomes absolute only after comparing different metals and creating their base.

1.2 Improved amplitude-phase model of response signal formation

Let us consider the processes that occur in the input cascades of the ECS we used for eddy current analysis of metals when scanning objects of control (OC) [3].

The signal at the input of the ECS phase detector can be represented as:

$$U_z = f \left[U_V(x, \mu_r, \sigma) \right].$$

If there is no OC in the area of operation of the antenna system, a signal with a frequency of ω . The instantaneous voltage value in the receiving antenna will be $U_{0Z} = U_{0Z\max}\cos(\omega t)$, where $U_{0Z\max}$ – the amplitude of the signal induced in the antenna.

In a previous work, an attempt was made to develop a signal model for an eddy current control system [14]. Taking into account the movement of the antenna over the metal OK, the instantaneous value of the signal at the receiving antenna can be written as:

$$U_Z = U_{1Z0} \cos\left(2\pi \frac{V}{L}t\right)\cos(\omega t + \varphi(t)),$$
 (1)

where $\varphi(t) = \varphi_{start} + \frac{\Delta \varphi}{\varphi_{\max}}t$, φ_{start} – initial phase shift value, φ_{\max} – maximum value of the initial phase shift, $\Delta \varphi$ – initial phase change step, U_Z – voltage in the receiving antenna taking into account the movement of the metal OC, U_{1Z0} – base voltage value on the antenna, V – linear velocity of movement of the metal

OC along the antenna turns, L – distance between the receiving and transmitting antennas.

At that time, studies were conducted using a loop antenna in the form of a double ring, where the receiving antenna is placed inside the transmitting antenna of a larger diameter in one plane, Fig. 2a. When a metal sample was carried over the plane of the antennas, the metal crossed the active zone twice, i.e. two arms. The current studies were conducted using a loop antenna, in which the edges of the transmitting (Tx) and receiving (Rx) antennas partially overlap each other and form a narrow active zone (L) and thus have only one working arm, $L=0.06\,\mathrm{m}$, Fig. 2b.

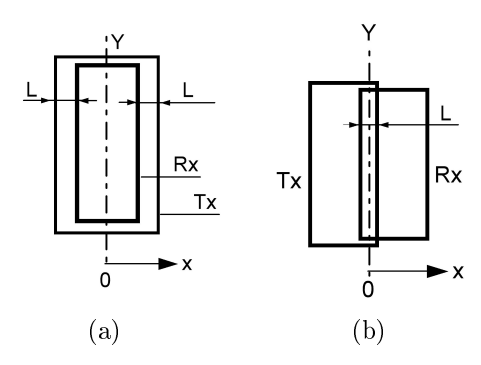


Fig. 2. Structural design of the loop antenna of the control system: (a) – two active zones, (b) – one active zone

Reducing the number of active arms and conducting a series of studies at different speeds of passing the sample over the antenna plane allowed us to reconsider the previously proposed signal model and make changes to it.

In the previously proposed model, the phase shift of the response signal, which is one of the informative coefficients, had to be measured separately experimentally. That is, the phase value was determined when the metal passed over several reference coordinates and this range between them was then divided by the number of points of the cosine. The graph was constructed by approximation, where for each iteration of the cosine, a separately measured phase value was substituted [11, 13]. This approach is not convenient due to the large time costs for signal modeling, and the model also did not take into account the magnetic permeability of the metal and dielectric conductivity.

When improving the signal model, the following physical effects were used:

- the occurrence of Foucault currents on the surface of a metal sample under the action of an alternating EM field [15];
- the phenomenon of mutual induction in a coil (loop antenna) when a charged body is passed over it according to Faraday's law;
- $-\operatorname{mechanical}$ modulation by rotating the metal over the antenna planes.

A correctly balanced antenna system [16,17] is such that a signal with a minimum amplitude of a few millivolts is transmitted from the transmitting antenna to the receiving antenna at a probe signal amplitude of 40 V. When a metal sample appears in the plane of the antennas, Foucault currents are induced on it, the balance between the antennas changes, and the signal level at the output of the receiving antenna changes [18,19].

According to Faraday's law of electromagnetic induction [20, 21], the electromotive force (EMF) is directly proportional to the rate of change of magnetic flux

$$\varepsilon = -N \frac{d\Phi}{dt},$$

where N – number of coil turns. The source of magnetic flux is a metal sample with eddy currents on its surface and rotating above the antenna planes. This important point was used in improving the signal model. Eddy currents are different due to the different magnetic and electrical properties of metals and their alloys [22, 23].

In this regard, the value of the initial phase of the alternating EM field appears in part of the formula [2]:

$$U_Z = U_{1Z0} \cos \left(2\pi \frac{V}{L}t + \varphi_{zm}(t)\right), \qquad (2)$$

where V is the linear transfer velocity of the metal sample, L this is the length of the active area of the antennas, i.e. V/L is the frequency of rotation of the metal sample above the coils, $\varphi_{zm}(t)$ – the phase of the alternating magnetic flux, which is proposed to be calculated from the influence function $\varphi_1(x,\beta)$ [2,7].

The influence function $\varphi_1(x,\beta)$ in non-destructive testing tasks is used to calculate the applied voltage in the receiving antenna, [2, 7] it takes into account the electrical and magnetic properties of metals:

$$\varphi_1(x,\beta) = \frac{\mu_r - \sqrt{x^2 + j\beta^2}}{\mu_r + \sqrt{x^2 + j\beta^2}},$$
(3)

where μ_r – relative magnetic permeability, $x = \lambda R_Z$, λ – integration parameter [1/m], $\beta = R_Z \sqrt{\omega \mu_a \sigma}$, σ – electrical conductivity of metal, μ_a – absolute magnetic permeability.

Since x is a location coordinate, for the task of developing a signal model, it is proposed to replace it with time references t, which allow us to calculate the value of the influence function when a metal sample is carried at different times, that is, at different coordinates.

Therefore, the modified version of the influence function has the following form:

$$\varphi_1(x,\beta) = \frac{\mu_r - \sqrt{t^2 + j\beta^2}}{\mu_r + \sqrt{t^2 + j\beta^2}}.$$
(4)

The process of induction of Foucault currents on the surface of a metal sample begins with the approach to the edge of the transmitting antenna, at the same time, the moving sample changes the EMF of the receiving antenna. The EMF reaches its maximum value when the sample is above the active zone of the antennas—their overlap plane. After overcoming this zone, the EMF begins to decrease. The change in the EMF

value in the time domain may have the form of a triangular function, possibly a Gaussian distribution function, possibly an exponential-like one, therefore, various forms of the envelope EMF were investigated in the signal model, Fig. 3. The EMF can be represented in a simplified way as a triangular one:

$$U_{ref}(t) = \begin{cases} U_{1Z0} \cdot ky & k = f(t); \ t = 0 \dots \frac{1}{2}T \\ U_{1Z0} \cdot (Ty - ky) & k = f(t); \ t = \frac{1}{2}T \dots T \end{cases}$$
(5)

where T is the time of transfer of the metal sample above the antenna plane, y is the gain coefficient.

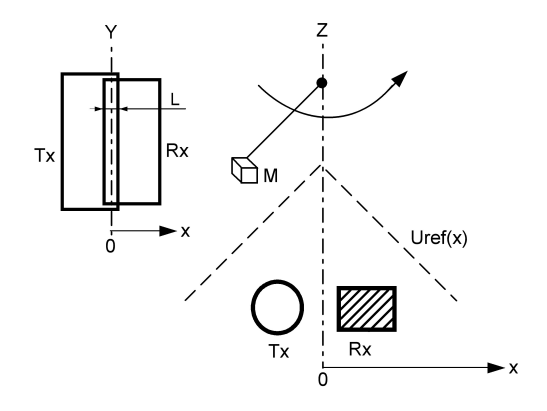


Fig. 3. The bypass EMF in a receiving antenna with one active zone

Thus, the improved signal model can be represented as:

$$U_Z = U_{ref} \cdot \cos(\omega t + \varphi(t)) \cdot \cos\left(2\pi \frac{V}{L}t + \varphi_{zm}(t)\right). \quad (6)$$

The envelope shape for an antenna with two active zones can be represented as the sum of two triangles that are overlapping each other, Fig. 4.

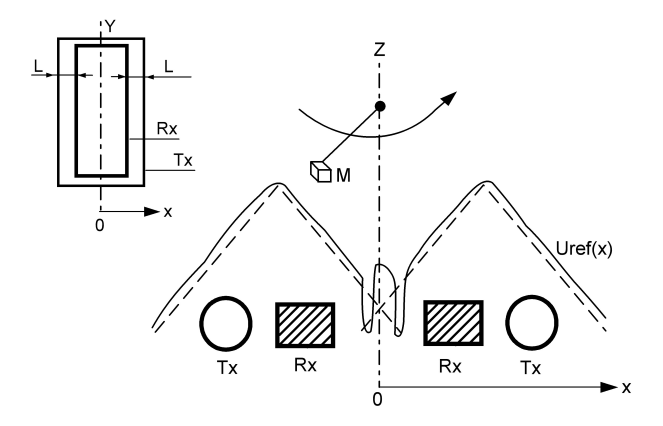


Fig. 4. The bypass EMF in a receiving antenna with two active zones

The simulated signals [24] for copper and steel are similar to those obtained experimentally: polarity of the first extremum, ratio between the extremes, Fig. 5-6.

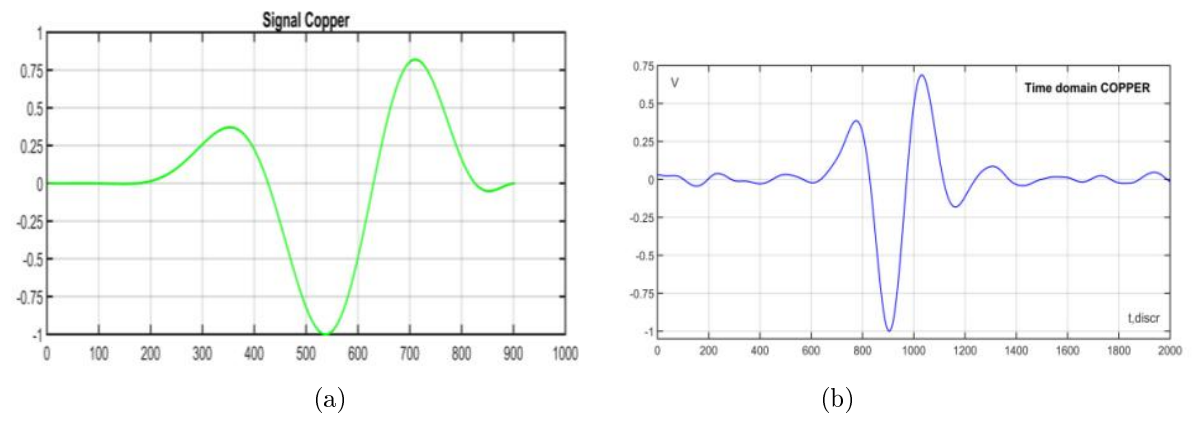


Fig. 5. Signal from a copper sample: (a) – simulated, (b) – experimentally measured

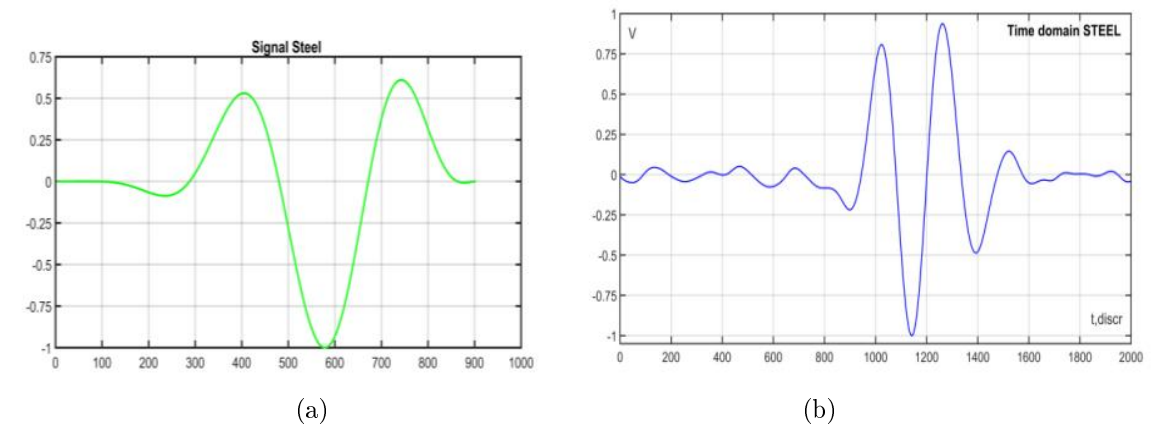


Fig. 6. Signal from a steel sample: (a) – simulated, (b) – experimentally measured

The signal model requires further study, because the shape of the envelope of the EMF value in the time domain is not known for certain [25]. When modeling in the Matlab environment, a triangular shape, a bell-shaped shape, and an exponential shape were tested, and all of them gave different ratios of signal extrema and the polarity of the first. Figures 5-6 shows the results for the bell-shaped envelope [26].

Nevertheless, the improved signal model has clear advantages:

- the value of the phase shift for a specific type of metal is calculated analytically, not by approximation;
- Lenz's law of mutual induction is taken into account and based on it, an envelope is added to the formula, which allowed us to obtain signals similar to the experimental ones.

From equation (6) it is clear that the speed of transferring the sample over the antenna planes is a factor influencing the shape of the response signal. At different speeds, the response signal has a different shape – it can stretch and decrease in amplitude at low speeds and gain a large amplitude and merge into one at high speeds. All this leads to the fact that the information coefficients about the response signal, which characterize a particular metal or alloy, will be

different and the correlation difference between them is also different.

Therefore, it is appropriate to determine the range of speeds that will be optimal in order to obtain the maximum mutual difference between the metals.

2 Experimental results and discussion

The response signal U is fed to the input of the analog-to-digital converter and is subsequently converted into a digital code and processed in the electronic unit using digital methods proposed in [2], which allows identifying the metal from which the control object is made [26].

The purpose of processing is to extract information coefficients that characterize a specific metal or alloy. These are their mutual ratio (K%), mean square difference between the amplitude of the head harmonic and others (KOP), the area of the spectrum under the envelope (S_{xs}) , the curvature of the envelope spectrum (E_{sym}) , the lower (f_n) and upper (f_v) limits of the spectra. They can be represented as a row matrix $f(K\%, E_{sym}, KOP, S_{xs}, f_n, f_v)$.

Schematically, the identification process can be represented as:

$$U(V, \sigma, \mu) \Rightarrow [\Phi] \Rightarrow f(K\%, E_{sym}, KOP, S_{xs}, f_n, f_v),$$

where Φ – a nonlinear filter, after passing through which information coefficients are extracted.

At different speeds of movement of the OC relative to the antenna, the signal shape will be different, accordingly the informative coefficients will also be different. The correlation of the coefficients with each other for different metals will lead to better or worse identification of them.

To study the problem of optimal speed, measurements were carried out with a frequency gradation from 10 to 18 Hz, with a step of 2 Hz (5 variations) [27, 28].

The resulting signal-response is characterized by six information coefficients [3]. When comparing the signal from an unknown sample with the signal from a known one, the percentage difference is calculated for each information parameter, the result is summed up and averaged. Accordingly, for two identical samples, the correlation discrepancy is 0%.

The classical analysis of finding extreme [11], which involves calculating the derivative with respect to one of the variables and equating the result to zero, is not acceptable because the criterion for maximum information between metals is the row matrix, not the initial function.

To find the optimal speed of movement of metal samples over the antenna, we suggest going the way of approximation – measuring information coefficients at different frequencies of rotation of the OC, and calculating the correlation discrepancy between metals at these frequencies. The greatest value of the correlation discrepancy will be at the optimal frequency – this will increase the correct identification of metals and alloys.

The calculation of the correlation difference can be represented as:

$$R_K = \frac{1}{n} \sum_{i=1}^{n} \left(\frac{P_1^i - P_2^i}{P_1^i} \cdot 100\% \right) \quad P_1^i > P_2^i, \tag{7}$$

where P_1, P_2 – the value of the parameters of each of the information features of the signal, n – number of information analysis parameters, n = 6.

It is important to note that the values of the weight coefficients for each of the 6 parameters are equal to 1, because determining the correct weight coefficients is a matter of further research.

Table 1 shows the values of the correlation difference of 20 different types of chemical elements at a rotation frequency of 14 Hz.

From Table 1 it can be seen that the correlation difference between metals and non-metals is significant, therefore it remains appropriate to determine the optimal frequency of rotation of the sample above the antenna.

To demonstrate the dependence of the correlation difference (ordinate axis) on the frequency (abscissa axis), a sample from the first row is taken and compared with 19 samples placed in the columns. That is, carbon and 19 other metals, steel and 19 other metals, cobalt and 19 other metals, etc. Different cases are shown in Fig. 7 – Fig. 8.

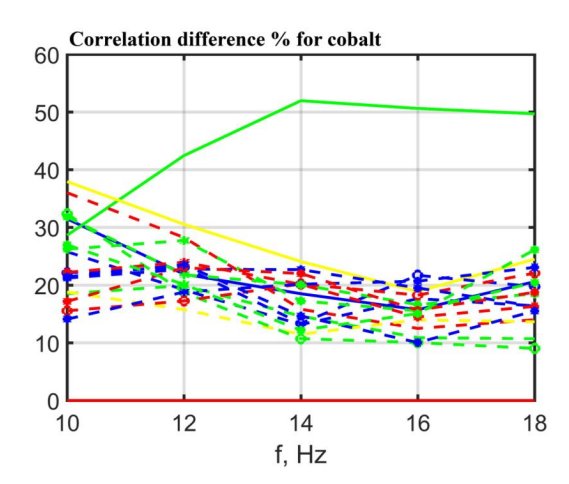


Fig. 7. Correlation difference from frequency for cobalt and other 19 elements

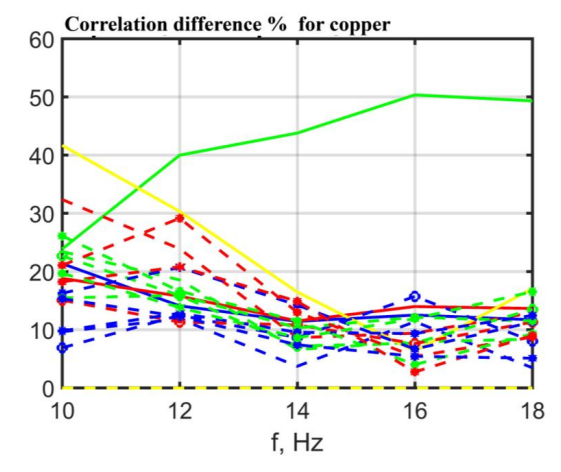


Fig. 8. Correlation difference with frequency for copper and other 19 elements

Analysis of the diagrams shows that there is no clearly defined optimal frequency, but there is a frequency range of 12...14 Hz, at which the maximum correlation integral characteristic is ensured.

The increase in signal amplitude with increasing rotation speed did not give a clear increase in the correlation difference between the coefficients, which is an unexpected result. At too high a frequency, the responses converge to one extremum, which can be explained by insufficient charging of the OC by the secondary field.

It should also be noted that the study and determination of weighting coefficients in future studies of each of the information parameters of the signal-response will give a more pronounced percentage difference in the samples between each other.

Table 1 Correlation difference values of different metals $\,$

	Part 1										
Nº	Correlation difference% metals	1	2	3	4	5	6	7	8	9	10
1	Carbon	0	45.34	18.53	16.11	12.46	7.20	16.95	11.45	11.81	14.02
2	graph Steel tab.	45.34	0	51.99	41.93	42.15	43.00	47.86	43.81	41.11	43.82
3	Cobalt	18.53	51.99	0	15.84	13.18	14.65	24.11	11.52	13.40	10.74
4	Magnesium	16.11	41.93	15.84	0	5.03	10.64	14.42	8.64	6.47	8.43
5	Duralumin	12.46	42.15	13.18	5.03	0	6.23	14.15	3.73	5.25	5.79
6	Vanadium	7.20	43.00	14.65	10.64	6.23	0	14.30	6.62	7.45	8.46
7	Chromium	16.95	47.86	24.11	14.42	14.15	14.30	0	16.49	16.31	16.28
8	Copper	11.45	43.81	11.52	8.64	3.73	6.62	16.49	0	8.65	7.20
9	Brass	11.81	41.11	13.40	6.47	5.25	7.45	16.31	8.65	0	4.83
10	Zinc	14.02	14.02	10.74	8.43	5.79	8.46	16.28	7.20	4.83	0
11	Zirconium	11.08	45.14	20.22	8.79	7.91	8.30	6.58	10.84	11.55	12.43
12	Molybdenum	12.64	47.02	22.71	13.44	12.52	12.82	4.65	14.25	14.64	14.14
13	Silver 999	7.64	45.18	17.29	13.09	9.50	6.12	13.95	10.34	8.19	8.91
14	Cadmium	20.36	44.13	20.15	6.33	10.19	15.31	11.14	13.00	10.82	12.66
15	Indium	7.80	47.02	20.18	13.30	10.75	8.73	9.95	9.57	15.16	15.71
16	Tin	12.63	47.08	20.09	11.56	10.57	10.69	6.15	11.54	12.81	10.84
17	Tantalum	16.93	46.31	22.03	13.66	12.28	11.27	7.27	14.90	14.12	14.07
18	Tungsten	7.50	43.86	14.67	11.12	6.65	3.51	15.56	7.42	6.45	7.56
19	Gold 999	13.25	46.90	12.20	16.08	11.39	10.88	23.60	8.64	11.57	9.85
20	Gold 900 (5r 1898y RI)	6.48	49.51	16.41	20.19	16.52	11.36	20.26	13.84	15.78	14.52
	Part 2					1				'	
Nº	Correlation difference% metals	11	12	13	14	15	16	17	18	19	20
1	Carbon	11.08	12.64	7.64	20.36	7.80	12.63	16.93	7.50	13.25	6.48
2	graph Steel tab.	45.14	47.02	45.18	44.13	47.02	47.08	46.31	43.86	46.90	49.51
3	Cobalt	20.22	22.71	17.29	20.15	20.18	20.09	22.03	14.67	12.20	16.41
4	Magnesium	8.79	13.44	13.09	6.33	13.30	11.56	13.66	11.12	16.08	20.19
5	Duralumin	7.91	12.52	9.50	10.19	10.75	10.57	12.28	6.65	11.39	16.52
6	Vanadium	8.30	12.82	6.12	15.31	8.73	10.69	11.27	3.51	10.88	11.36
7	Chromium	6.58	4.65	13.95	11.14	9.95	6.15	7.27	15.56	23.60	20.26
8	Copper	10.84	14.25	10.34	13.00	9.57	11.54	14.90	7.42	8.64	13.84
9	Brass	11.55	14.64	8.19	10.82	15.16	12.81	14.12	6.45	11.57	15.78
10	Zinc	12.43	14.14	8.91	12.66	15.71	10.84	14.07	7.56	9.85	14.52
11	Zirconium	0	6.11	8.55	12.25	5.21	3.90	8.82	9.65	18.20	14.75
12	Molybdenum	6.11	0	11.97	9.73	5.70	4.22	7.20	13.42	21.59	16.14
13	Silver 999	8.55	11.97	0	16.91	11.71	8.57	12.45	3.82	11.62	9.70
14	Cadmium	12.25	9.73	16.91	0	14.06	12.02	11.27	15.59	20.49	24.43
15	Indium	5.21	5.70	11.71	14.06	0	5.91	10.94	11.56	17.18	11.52
16	Tin	3.90	4.22	8.57	12.02	5.91	0	7.32	10.59	18.32	14.79
17	Tantalum	8.82	7.20	12.45	11.27	10.94	7.32	0	12.80	20.63	20.19
18	Tungsten	9.65	13.42	3.82	15.59	11.56	10.59	12.80	0	9.87	10.70
19	Gold 999	18.20	21.59	11.62	20.49	17.18	18.32	20.63	9.87	0	7.94
20	Gold 900 (5r 1898y RI)	14.75	16.14	9.70	24.43	11.52	14.79	20.19	10.70	7.94	0

Conclusions

The article considers the signal-response model of the eddy current dynamic control method system. The considered aspects of the dynamic control process implementation allowed us to improve the previously proposed signal-response model, thanks to which it now takes into account the electrical and magnetic characteristics of metals analytically, and not by approximate substitution as in the previous model. An important part of the model is the shape of the envelope of the process of the emergence of a secondary electromagnetic field on the surface of a metal object and its attenuation, which occurs during dynamic control, namely when the metal object is carried over the plane of the antennas. Determining the correct shape of the envelope in the future will allow obtaining theoretical signals more similar to experimental ones.

When performing the simulation, the variable is the speed of the metal object passing over the antenna plane. The speed affects the shape of the response signal and the information coefficients calculated later.

Considering that the weighting coefficients are taken equal to 1, the obtained results showed that the optimal is not a single rotation frequency, but the results of metal identification from the range of rotation frequencies within 12-14 Hz, which corresponds to the range of linear speeds of 4...6 m/s.

Metal identification using several different frequencies is better and more accurate, as it allows for a more informative characterization of an unknown new sample and to determine which ones it is most similar to.

Conducting research to determine the optimal rotation frequency of metal objects above the antenna plane allowed to increase the efficiency when distinguishing metals due to the increase in the correlation difference in the example of copper and other metals from 10-15% to 20-25%, in the example of tantalum from 8-12% to 15-20%, and in the case of cobalt from 10-12% to 20%.

Thus, an improved signal-response model and determination of the range of rotation speeds of a metal sample above the antenna planes to increase the efficiency allow us to further investigate the issue of controlling those metal surfaces and samples to which there is currently no physical access.

References

- [1] Positive Material Identification. *Elvatech Ltd*. Available online, data access: june 2025.
- [2] Abramovych, A. O., Agalidi, Y. S., Piddubnyi, V. O. (2020). Radio engineering system identification of metals on the basis of eddy-current converters. *Radio Electro*nics, Computer Science, Control, No. 1, pp. 7-17. doi:10.15588/1607-3274-2020-1-1.
- [3] Abramovych A. O. (2022). Improving the eddy current identifier of metals based on the correlation approach.

- Radio Electronics, Computer Science, Control, No. 4, pp. 7-17. doi:10.15588/1607-3274-2022-4-1.
- [4] Bruschini C. (2002). A Multidisciplinary Analysis of Frequency Domain Metal Detectors for Humanitarian Demining: thesis dissertation of Doctor in Applied Sciences. Vrije Universiteit Brussel, 242 p.
- [5] Peyton, A. J., Verre, W. V., Gao, X., Marsh, L. A., Podd, F. J. W., Daniels, D. J., Ambruš, D., Vasić, D., Bilas, V. (2019). Embedding target discrimination capabilities into handheld detectors for humanitarian demining. In: *The 16th International Symposium Mine Action*, pp. 31–35. Ministry of Science and Education, Zagreb.
- [6] Daniels, D. J. (2004). Ground Penetrating Radar (2nd Edition). *Institution of Electrical Engineers*, London, UK, 761 p. DOI:10.1049/pbra015e.
- [7] Sharawi M. S. and Sharawi M. I. (2007). Design and Implementation of a Low Cost VLF Metal Detector with Metal-Type Discrimination Capabilities. 2007 IEEE International Conference on Signal Processing and Communications, pp. 480-483, doi:10.1109/ICSPC.2007.4728360.
- [8] Abramovych, A. A., Kashirsky, I. S., & Poddubny, V. A. (2017). Method of processing the reflected signals from pulsed eddy current converters. *Radio Electro*nics, Computer Science, Control, Vol. 4, pp. 7-14. doi:10.15588/1607-3274-2017-4-1.
- [9] Tietze U., Schenk Ch. (2019). Halbleiter-Schaltungstechnik.
 Springer Vieweg; 16th, adult, Updated edition, 1828 p. ISBN 978-3662485538.
- [10] Method and apparatus for metal detection employing digital signal processing. (2008). *United States Patent*, Patent No.: US 7,432,715 B2. Data of Patent Oct. 7, 2008.
- [11] Ifeachor, E. C.; Jervis, B. W. (2001). Digital Signal Processing: A Practical Approach, 2nd Edition, Hoboken, USA: Prentice Hall; 933p. ISBN 978-0201596199.
- [12] Salih M. (2012). Fourier Transform Signal Processing. Intech Open, 366 p. Doi: 10.5772/813.
- [13] Stroustrup B. (2014). Programming: principles and practice using C++ (2nd Edition). Addison-Wesley, 2339 p., ISBN 978-0321-992789.
- [14] Abramovych A. O., Poddubny V. O. (2020). Eddy-Current Amplitude-Phase Based Method for Identifying Conductive (Metal) Objects. *Metallofiz. Noveishie Tekhnol.*, Kyiv, Vol. 42, No.8, pp. 1069-1085. DOI: 10.15407/mfint.42.08.1169.
- [15] Yamazaki, S.; Nakane, H.; Tanaka, A. (2002). Basic Analysis of a Metal Detector. *IEEE Trans. Instrumentation and Measurement*, Vol. 51, Iss. 4, pp. 810-814. DOI: 10.1109/TIM.2002.803397.
- [16] Potin, D.; Vanheeghe, P.; Duflos, E.; Davy, M. (2006). An abrupt change detection algorithm for buried landmines localization. *IEEE Transactions on Geoscience and Remote Sensing*, Vol. 44, No. 2, pp. 260-272, doi:10.1109/TGRS.2005.861413.
- [17] Bermani, E.; Boni, A.; Caorsi, S.; Massa, A. (2003). An innovative real-time technique for buried object detection. *IEEE Trans. Geosci. Remote Sens.*, Vol. 41, Iss. 4, pp. 927-931. DOI: 10.1109/TGRS.2003.810928.
- [18] AN/PSS-14 (former HSTAMIDS) mine detector, L-3 CyTerra. L3 Harris. Available online, data access: june 2025.
- [19] Minehound VMR3G, Dual sensor mine detector. Vallon GmbH. Available online, data access: june 2025.

- [20] Jol, M. H. (2009). Ground Penetrating Radar. Theory and Applications. *Elsevier Science*; 574 p. DOI:10.1016/B978-0-444-53348-7.X0001-4.
- [21] Daniels, D. J. (2009). EM Detection of Concealed Targets. John Wiley & Sons; 299 p. DOI:10.1002/9780470539859.
- [22] Moore, P. O. (2004). *Electromagnetic testing*. Columbus, USA: American society for nondestructive testing; 529 p.
- [23] Bristow, C. S.; Jol H. M. (2003). Ground Penetrating Radar in Sediments. Birkbeck, University of London, UK; 339 p.
- [24] Electromagnetic method of identification of metals: invention patent 127276 Ukraine: G01N 27/90. № u 2020 08222; info. 22.12.2020; printed. 05.07.2023, journal. № 27/2023.
- [25] Yamazaki T., Arizono T., Kobayashi T., Ikuta R., Yamamoto T. (2023). Linear Optical Quantum Computation with Frequency-Comb Qubits and Passive Devices. *Physical Review Letters*, Vol. 130, 200602, pp. 200602-1-200602-6, doi:10.1103/PhysRevLett.130.200602.
- [26] Lewis, E. E., Sahay, C. & Breneman, J. E. (2022). Introduction to Reliability Engineering, 3rd Edition. Wiley & Sons.
- [27] Chekubasheva V. A., Kravchuk O. A., Hlukhova H., Glukhov O. V. (2022). Creating of a remotepresence robot based on the development board Texas Instruments to monitor the status of infected patients. Biosensors and bioelectronics: X, Vol. 11, 100215. DOI:10.1016/j.biosx.2022.100215.
- [28] Shi B. et al. (2022). Impact of Low-Resolution ADC on DOA Estimation Performance for Massive MIMO Receive Array. *IEEE Systems Journal*, Vol. 16, Iss. 2, pp. 2635-2638, doi: 10.1109/JSYST.2021.3139449.

Удосконалення системи вихрострумового контролю та моделі аналізу сигналу відгуку для збільшення інформативності при ідентифікації металів

Абрамович А. О., Баженов В. Г.

В роботі розглядаються результати ідентифікації металевих об'єктів за допомогою вихрострумової системи динамічного контолю, на базі амплітудно-фазового методу обробки відгуку від об'єкта, що досліджується. В статті запропонована удосконалена модель сигналувідгуку вихрострумової системи динамічного методу контролю. Враховані аспекти здійснення процесу динамічного контролю дозволили удосконалити запропоновану раніше аналітичну модель опису сигналувідгуку, завдяки чому вона тепер враховує електричні та магнітні характеристики металів аналітичним шляхом, а не апроксимаційним підставленням форми сигналувідгуку, як попередня модель.

В роботі акцентовано увагу, що важливою змінною моделі є швидкість пронесення металевого предмета над площиною антен. Швидкість впливає на форму сигналу-відгуку та розрахованих в подальшому інформаційних коефіцієнтів. Проведено дослідження із визначення оптимальної швидкості пронесення металевого предмета над поверхнею антен, що відповідає діапазону лінійних швидкостей $4\dots 6\,$ м/с.

Ідентифікація металів при використанні кількох різних частот обертання є кращою та точнішою, адже дозволяє більш інформативно охарактеризувати невідомий новий зразок та визначити до яких він є максимально подібним.

Проведення досліджень по визначенню оптимальної частоти обертання металевих предметів над площиною антен дозволило збільшити інформативність системи, про що свідчило зростання кореляційної різниці при розрізненні металів на прикладі міді та решти металів з 10-15% до 20-25%, на прикладі танталу з 8-12% до 15-20%, а кобальту з 10-12% до 20%.

Ключові слова: електромагнітні властивості металів; вихрострумова система; STM32H745 мікроконтролер; модель сигналу-відгуку; ідентифікація металів; математичне моделювання; амплітудно-фазовий метод реєстрації сигналів; інформативність; STM32; металошукач